Mon. Not. R. Astron. Soc. **000**, 000–000 (0000) Printed 7 May 2002 (MN LaTeX style file v1.4)

First X-ray observations of the polar CE Gru

Gavin Ramsay and Mark Cropper
Mullard Space Science Lab, University College London, Holmbury St. Mary, Dorking, Surrey, RH5 6NT, UK

ABSTRACT

We report the detection of the polar CE Gru in X-rays for the first time. We find evidence for a dip seen in the hard X-ray light curve which we attribute to the accretion stream obscuring the accretion region in the lower hemisphere of the white dwarf. The X-ray spectrum can be fitted using only a shock model: there is no distinct soft X-ray component. We suggest that this is because the reprocessed component is cool enough so that it is shifted into the UV. We determine a mass for the white dwarf of $\sim 1.0 M_{\odot}$.

Key words: Stars: individual: CE Gru – Stars: binaries – Stars: cataclysmic variables – X-rays: stars

1 INTRODUCTION

CE Gru (also known as Grus V-1 and Hawkins V-1) was discovered by Hawkins (1981, 1983) during a search for variable objects using UK Schmidt plates. Further observations by Tuohy et al (1988) confirmed its binary nature (an orbital period of 108.5 mins) while Cropper et al (1990) found strong circular polarisation – a characteristic of the polar (or AM Her) class of cataclysmic variable. These objects are interacting binaries in which material flows from a dwarf main sequence star onto a magnetic (B ∼10–200MG) white dwarf. This strong magnetic field is high enough to force the spin of the white dwarf to be synchronised with the binary orbital period.

Tuohy et al (1988) demonstrated that there are two accretion poles which are characterised by different emission properties: one pole which is always in view and is stronger in blue light, while the other pole which is visible for only ∼0.35 of the white dwarf spin period is stronger in red light. Cropper et al (1990) showed that the pole always in view was positively circularly polarised, with the other being negatively polarised.

The UK Schmidt plates show that CE Gru exhibits two distinct levels of brightness, (B ∼18 and B ∼21). In the fainter state the accretion flow is much reduced, or stopped altogether. This may be the reason why CE Gru was not detected during the *ROSAT* all-sky survey (Verbunt et al 1997). Indeed, CE Gru has never before been detected in X-rays. In this paper, we report the first X-ray detection of CE Gru which were made as part of a survey of polars using *XMM-Newton*.

2 OBSERVATIONS

The satellite *XMM-Newton* was launched in Dec 1999 by the European Space Agency. It has the largest effective area of any X-ray satellite and also has a 30 cm optical/UV telescope (the Optical Monitor, OM: Mason et al 2001) allowing simultaneous X-ray and optical/UV coverage. CE Gru was observed using *XMM-Newton* on 2001 Oct 31. The EPIC instruments (imaging detectors covering the energy range 0.1–10keV with moderate spectra resolution) were operated in full frame mode (the count rate was not high enough to cause pile-up problems). The RGS detectors (high resolution spectrographs operating in the 0.3–2.0keV range: den Herder et al 2001) were configured in the standard spectroscopy mode. We clearly detect CE Gru in the X-ray band. OM data were taken in two UV filters (UVW1: 2400–3400 Å, UVW2: 1800–2400 Å) and one optical band (V band). The observation log is shown in Table 1.

The data were processed using the *XMM-Newton Science Analysis Software* v5.2. The RGS spectra were of low signal to noise and showed no evidence for significant line emission: we do not consider them further. For the EPIC pn detector (Strüder et al 2001), data were extracted using an aperture of $40''$ arc sec centered on the source. Background data were extracted from a source free region. For the EPIC MOS detectors (Turner et al 2001) we extracted data in a similar way, but extracted the background from an annulus around the source. The background data were scaled and subtracted from the source data. In extracting the EPIC pn spectrum, we used only single pixel events and used the response file epn_ff20_sY9_thin.rmf. In the case of the MOS data we used the response files m[1-2]_thin1v9q19t5r5_all_15.rsp. The OM data were analysed in a similar way using `omichain` and `omfchain` (this latter task

Detector	Mode	Filter	Exp (s)
EPIC MOS	Full frame	thin	7792
EPIC pn	Full frame	thin	5468
RGS	Spectroscopy		8255
OM	Image/fast	UVW1	1500
OM	Image/fast	V	1500
OM	Image/fast	UVW2	1800

Table 1. The log of *XMM-Newton* observations of CE Gru.

was not incorporated in SAS v5.2 but will be in a later version). Data were background subtracted and corrected for coincidence losses (Mason et al 2001).

The Optical Monitor data shows that CE Gru had a mean brightness of V=17.9 and a maximum V=17.5. Since the V band observations started at the descent from maximum its likely that its true maximum was brighter than this. Assuming a similar colour to that found by Tuohy et al (1988) ($B-V$=0.53) this places CE Gru in a high accretion state at the time of the *XMM-Newton* observations and a similar brightness to observed by Tuohy et al ($V\sim$18). The length of the observation in the EPIC MOS detectors covered just over 1 orbital cycle.

The flux in the UV filters corresponds to: UVW1 $\sim$ 4.5×10^{-16} ergs s^{-1} cm^{-2}Å, UVW2 $\sim$ 4.0×10^{-16} ergs s^{-1} cm^{-2}Å, (based on OM observations of isolated white dwarfs). The mean flux in the V filter corresponds to $\sim$ 2.5×10^{-16} ergs s^{-1} cm^{-2}Å at 5000 Å.

3 LIGHT CURVES

We show in Figure 1 the light curve of CE Gru in various energy bands using EPIC pn and EPIC MOS data (where the MOS1 and MOS2 data have been co-added) folded on the orbital period of Tuohy et al (1988). We also show the OM data: CE Gru was detected in all three filters (it is also the first time that it has been detected in the near-UV).

There are two distinct parts to the orbital light curve: a faint phase lasting $\sim$ 0.6 orbital cycles, and a brighter phase lasting $\sim$ 0.4 orbital cycles. These relative durations are similar to those in the optical light curves seen by Cropper et al (1990). The bright phase is also of a similar duration to that of the red pole seen by Tuohy et al (1988) when the system was at a similar brightness compared to our observations. We therefore assign the bright phase X-ray emission to the pole in the lower hemisphere, and the fainter phase emission to the pole in the upper hemisphere. Although there maybe some ambiguity in this assignment, the fact the we observe decreasing emission in the V band at the end of the bright phase provides supporting evidence for this assignment since the 'blue' pole does not show such a rapid drop in V.

In the bright phase, a dip is seen in the soft X-ray light curve, but not at higher energies. This is characteristic of photo-electric absorption, and is seen in other polars (eg Watson et al 1989). It is thought to result from the accretion stream crossing our line of sight to the accretion region, thereby absorbing the soft X-rays. This is consistent with the model of Wickramasinghe et al (1991) for CE Gru in which the two accretion regions lie near the magnetic poles,

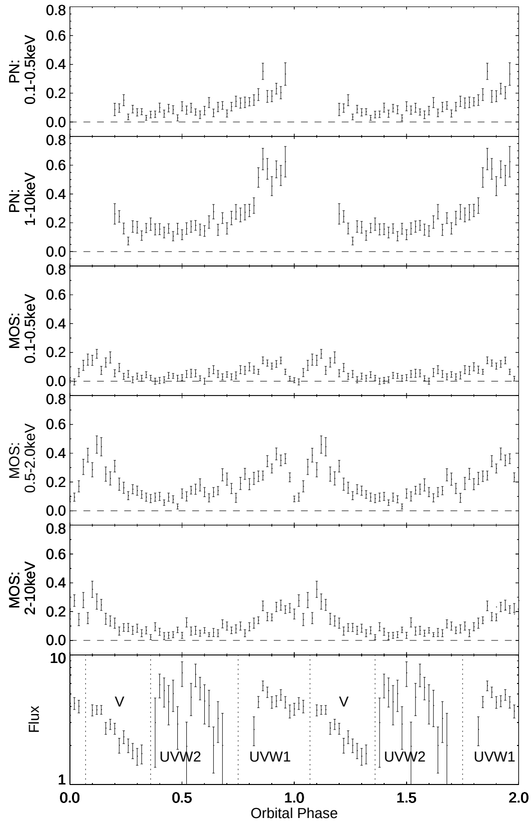

Figure 1. The light curves obtained of CE Gru using *XMM-Newton*. The X-ray data were obtained using the EPIC pn and MOS detectors. The MOS1 and MOS2 light curves have been co-added. The Optical Monitor data (bottom plot) shows the optical/UV data with units of flux of 10^{-16} ergs s^{-1} cm^{-2}. The data have been phased on the orbital period of Tuohy et al (1988) and binned into $\delta\phi$ =0.02 bins. We have chosen phase 0.0 to correspond to the dip centered in the bright phase.

approximately at the foot-points of the field lines passing through the region where the stream threads onto the magnetic field. It is most likely that the dip is caused by the accretion stream to the *upper* pole absorbing the emission from the lower pole: there is clear evidence for accretion at the upper pole and it is inevitable that the stream crosses our line of sight. It is possible for the ballistic stream or the stream to the lower pole to be the cause of the absorption, but this requires a high inclination and the ballistic stream to penetrate very close to the white dwarf before threading. These are special conditions, and in the absence of even a grazing eclipse we consider this to be unlikely.

At energies greater than 2keV, there is no evidence for the dip seen at lower energies. Using the spectral model described below we can estimate the absorbing column density of the accretion stream which causes the dip by increasing the column until we match the observed count rate at lower energies. We estimate that the total column density in our line of sight must be $\sim 5-10\times10^{21}$ cm^{-2}. This is of the same order as that seen in other polars with stream dips (Watson et al 1989).

4 X-RAY SPECTRA

4.1 The model

We extracted a faint and bright phase spectrum (ϕ=0.2–0.8 and ϕ=0.8–1.2 respectively) from the EPIC MOS data and a faint phase spectrum from the EPIC pn data (these data covered too short a length of time to obtain a useful bright phase spectrum). We modelled the data using a simple neutral absorber and an emission model of the kind described by Cropper et al (1999). This emission model, unlike single temperature thermal bremsstrahlung models, is a realistic physical description of the post-shock accretion region in polars. It is based on the prescription of Aizu (1973) which predicts the temperature and density profiles over the height of the accretion shock. However, it has been modified to take into account cyclotron cooling (which can be significant in polars) and also the variation in gravitational force over the shock height. To reduce the number of free parameters we fix the parameter, ϵ_s, (the ratio of cyclotron cooling to thermal bremsstrahlung cooling), at 5: this implies a magnetic field strength typical of polars (20–50MG). We also fix the specific accretion rate at 5 g s^{-1} cm^{-2} (typical of polars in a high accretion state). Changing these parameters does not have a great effect on the results for data with low-moderate signal to noise ratio (as in our CE Gru data). Observations of polars using *ROSAT* showed that many polars had prominent blackbody components (Ramsay et al 1994). Therefore, we also added a cool blackbody model and determined the change in the fit.

4.2 Results

We initially consider the EPIC spectra from the faint state. We show in Table 2 the fits to the MOS and pn spectra (we fit the MOS spectra simultaneously while leaving their normalisation parameters untied). We find that the spectrum can be well modelled without a blackbody component. The Hydrogen column density is low ($< 10^{20}$ cm^{-2}). Adding a blackbody to the model makes no significant difference to the fit. We do, however, show in Table 2 the fit and flux when we add a blackbody of temperature 30eV (typical of the temperature of the blackbody component seen in *ROSAT* observations of polars) to the model. In the bright phase data, again we find no significant improvement to the fit when we add a blackbody to the model. We show in Figure 2 the EPIC MOS1 spectra taken from the bright and faint phase, together with the best fits (assuming no blackbody).

Table 2 shows that the inferred mass of the white dwarf (assuming the white dwarf mass-radius relationship of Nauenberg 1972) is $\sim$1.0$M_\odot$. Although this is higher than found for isolated white dwarfs, it is comparable with the mass of other accreting magnetic white dwarfs. Ramsay (2000) show that the latter class are biased towards higher masses.

4.3 Soft and hard luminosities

We define the hard X-ray luminosity as ($L_{hard} = 4\pi \mathrm{Flux}_{hard,bol} d^2$) where Flux$_{hard,bol}$ is the unabsorbed, bolometric flux from the hard component and d is the distance. Since a fraction of this flux is directed towards the observer, we switch the reflected component to zero after the final fit to determine the intrinsic flux from the optically thin post-shock region. We define the soft X-ray luminosity as ($L_{soft} = \pi \mathrm{Flux}_{soft,bol} \sec(\theta) d^2$), where we assume that the soft X-ray emission is optically thick and can be approximated by a small thin slab of material, the unabsorbed bolometric flux is Flux$_{soft,bol}$ and θ is the mean viewing angle to the the accretion region.

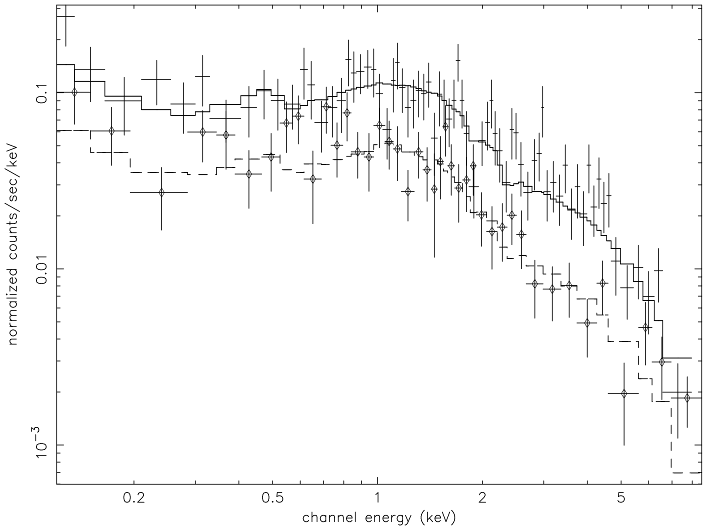

Figure 2. The EPIC MOS1 spectra extracted from the bright phase (dots) and the faint phase (diamonds) data together with a multi-temperature shock model (solid line for the bright phase and dashed line for the faint phase).

The is some degree of uncertainty in the viewing angle to the accretion regions. Tuohy et al (1988) found $i \sim 40^\circ$ and the red pole (the bright X-ray pole) has $\beta \sim 125^\circ$ and the blue pole (the faint X-ray pole), $\beta \sim 40^\circ$. More detailed modelling of Cropper et al (1990) and Wickramasinghe et al (1991) find $i \sim 40^\circ$, a dipole offset of 165° and the red pole displaced from the magnetic pole by $\sim 30^\circ$ and the blue pole $\sim 150^\circ$. However, the blue accretion region (the faint X-ray region) is seen for all spin phases (and hence a relative small viewing angle) and the red region for only a small fraction of the spin phase (and hence at a high viewing angle). For argument we apply a mean viewing angle of θ=60° (implying secθ=2.0) for the faint phase and θ=80° (secθ=5.8) for the bright phase.

We show in Table 2 the resulting luminosities for the shocked component (the 'hard' component) and the blackbody component assuming kT_{bb}=30eV. We find that the ratio, L_{soft}/L_{hard}, in the faint phase is very low, with an upper limit of $\sim$0.1. In the bright phase, the upper limit is 0.7. In the standard accretion model, hard X-rays in the post-shock region irradiate the photosphere of the white dwarf and are re-emitted at lower energies. Assuming the re-processed component is emitted in soft X-rays, we expect $L_{soft}/L_{shock} \sim 0.5$ (Lamb & Masters 1979, King & Lasota 1979). The total shock luminosity is the sum of hard X-ray emission and the emission from the cyclotron component which originates from the post-shock flow as well. Therefore, L_{hard} underestimates L_{shock}.

	Faint Phase EPIC MOS	EPIC pn	Bright Phase EPIC MOS
N_H (10^{20} cm^{-2})	$0.0^{+1.3}$	$0.0^{+0.04}$	$0.0^{+0.02}$
M_1 ($M_\odot$)	$1.04^{+0.18}_{-0.23}$	$1.03^{+0.18}_{-0.15}$	$1.29_{-0.15}$
Flux$_{hard,bol}$ (ergs s^{-1} cm^{-2})	$2.1^{+0.9}_{-0.6}\times10^{-12}$	$2.2^{+0.5}_{-0.3}\times^{-12}$	$7.1^{+0.8}_{-1.0}\times10^{-12}$
	$2.1^{+1.0}_{-0.6}\times10^{-12}$		$8.2^{+0.2}_{-1.4}\times10^{-12}$
$L_{hard,bol}$ (ergs s^{-1} d_{100}^2)	$2.5^{+1.1}_{-0.7}\times10^{30}$	$2.7^{+0.5}_{-0.4}\times10^{30}$	$9.1^{+0.2}_{-1.8}\times10^{30}$
	$2.6^{+1.2}_{-0.7}\times10^{30}$		$1.0^{+0.1}_{-0.2}\times10^{31}$
χ^2_ν(dof)	1.07 (82)	1.08 (104)	0.92 (143)
+ bb (eV)	30	30	30
Flux$_{soft,bol}$ (ergs s^{-1} cm^{-2})	$1.5^{+1.2}_{-1.5}\times10^{-13}$	$1.9^{+17}_{-1.9}\times10^{-13}$	$1.1^{+2.0}_{-1.1}\times10^{-12}$
	$1.5^{+1.2}_{-1.5}\times10^{-13}$		$8.9^{+14.6}_{-8.9}\times10^{-13}$
$L_{soft,bol}$ (ergs s^{-1} d_{100}^2)	$9.0^{+1.8}_{-9.0}\times10^{28}$	$1.1^{+1.7}_{-1.1}\times10^{29}$	$1.9^{+3.5}_{-1.9}\times10^{30}$
	$9.0^{+1.8}_{-9.0}\times10^{28}$		$1.6^{+2.5}_{-1.6}\times10^{30}$
χ^2_ν(dof)	1.06 (79)	1.07 (103)	0.90 (140)

Table 2. The parameters for the EPIC spectra extracted from the faint phase and bright phase. The MOS1 and MOS2 spectra were fitted simultaneously with all the parameters linked except the normalisations. We also show the effect on the fit if we add a blackbody with kT_{bb}=30eV to the model.

In the faint phase, it is clear that for a blackbody of temperature 30eV, the resulting energy balance is not consistent with the standard shock model. However, lower temperature blackbodies can be 'hidden' at EUV wavelengths. To investigate this further, we added a blackbody component of different temperatures and set their normalisation so that the derived flux matched that observed in the UVW2 filter. We show the model of the combined blackbody plus post-shock model in Figure 3 for kT_{bb}=2, 5, 10 and 20eV. We also show in Table 3 the fit to the data for these models in the 0.1–1.0keV band, the resulting flux and luminosity for the unabsorbed blackbody. We find that the observed X-ray spectra are not consistent with blackbody temperatures greater than ~10eV.

The un-heated surface of the white dwarf is also expected to contribute to the flux seen in the UV. However, we do not know its temperature (but it is expected to be near 1–2eV ~10000-20000K) nor do we have an accurate estimate of its distance. Because of these uncertainties we do not add a blackbody to account for this component: ~10eV is therefore an approximate upper-limit to the temperature of the reprocessed component. For kT_{bb}=10eV the resulting L_{soft}/L_{hard} ratio (~9) is very much greater than that expected from the standard accretion shock model but for kT_{bb}=5eV it is slightly higher than expected (~1.6). For lower temperatures (2eV) the ratio is slightly lower than that expected.

4.4 The distance

In the bright phase the hard X-ray bolometric luminosity is $\sim 1\times10^{31}$ ergs s^{-1} d_{100}^2. To place a very crude estimate on the distance to CE Gru we compare this luminosity to the hard X-ray luminosity of AM Her (whose distance is reasonably well determined). Ishida et al (1997) observed AM Her using *ASCA* when it was in a high accretion state and find $L_{hard}=1.6\times10^{32}$ ergs s^{-1}using a distance of 75 pc. We find that CE Gru would have to lie ~400 pc distance to equal the L_{hard} found for AM Her.

kT_{bb} (eV)	χ^2_ν (dof)	Blackbody flux (ergs s^{-1} cm^{-2})	Blackbody luminosity (ergs s^{-1} d_{100}^2)	$L_{soft}/$ L_{hard}
20	4.31 (27)	2.68×10^{-10}	1.6×10^{32}	64
10	1.39 (27)	3.86×10^{-11}	2.2×10^{31}	9.0
5	1.43 (27)	6.70×10^{-12}	4.0×10^{30}	1.6
2	1.44 (27)	1.34×10^{-12}	8.0×10^{29}	0.3

Table 3. Using the MOS spectra from the faint phase we have added a blackbody of various temperatures: the normalisation has been set to give the observed flux in the UVW2 filter. We show the resulting fit to the X-ray data in the 0.1–1.0keV band, the unabsorbed bolometric flux and luminosity of the blackbody component and the ratio L_{soft}/L_{hard} (cf Table 2).

5 DISCUSSION

Although CE Gru was detected in X-rays for the first time and was clearly in a high accretion state, no distinct soft X-ray component was observed. On the face of it, this is surprising since a strong soft X-ray flux has long been considered one of the defining properties of polars. Observations of polars using *EXOSAT* (eg Osborne 1988) and *ROSAT* (eg Ramsay et al 1994) found a strong distinct soft X-ray component, and in general, the ratio $L_{soft}/L_{hard}\gg1$. Further, the ratio was correlated with the magnetic field strength of the white dwarf: a high field gave a high ratio. To account for the large 'soft X-ray excess' seen in many polars, dense 'blobs' of material which do not form a shock and radiate in soft X-rays were proposed (Kuijpers & Pringle 1982, Frank, King & Lasota 1988).

Currently, four polars have been observed using *XMM-Newton*. Of those systems observed in an intermediate or high accretion state, WW Hor showed no distinct soft X-ray component (Ramsay et al 2001) while BY Cam has one pole which did show such a component and one which did not (Ramsay & Cropper 2002). Indeed only one other system, DP Leo, has shown a distinct soft X-ray component (Ramsay et al 2001). Even for those polars which showed the lowest

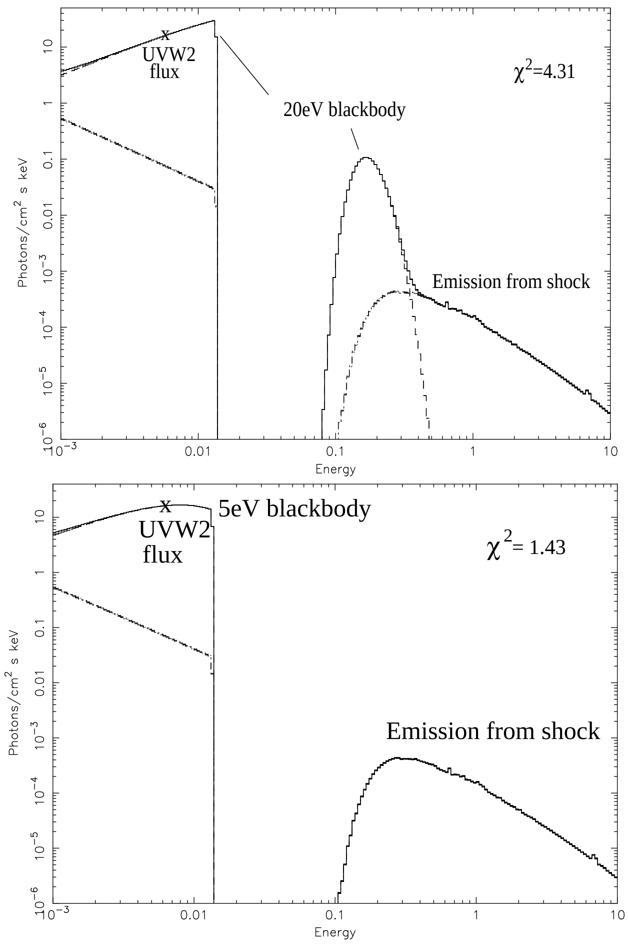

Figure 3. We show the best fit shock model that was used to fit the EPIC MOS1 data in the faint phase together with a blackbody of various temperatures. The normalisation of the blackbody was chosen to fit the observed flux in the UVW2 filter. A reprocessed component with less than kT_{bb} ~10eV is therefore be cool enough not to be detected in the X-ray band.

ratios using *ROSAT* (EF Eri and AM Her) a distinct soft X-ray component was still observed.

A variation of the standard shock model has been proposed by Heise & Verbunt (1988) and Gänsicke, Beuermann & de Martino (1995) who suggest that the reprocessed X-ray component lies in the EUV band while the strong soft X-ray component seen in many polars originates from dense 'blobs' of material which do not form an exposed shock. Our data are consistent with this view if the temperature of the reprocessed component is $\sim 2-5$eV: below 2eV the flux of the reprocessed component is too small, while above 5eV it would be too high. A component with a temperature above 10eV would be evident in the spectrum (Figure 3). The implication in this case is that the fraction of blobby accretion is small in CE Gru. Again this is consistent with the unfolded light curves (not shown) which do not show strong flaring seen in many systems (such as BY Cam – Ramsay & Cropper 2002).

The amount of irradiation that the white dwarf receives is a function of height in the post-shock region, with greater temperatures from higher up, but more overall flux (even at higher energies) from near the base (Cropper, Wu & Ramsay 2000). On the other hand, because of the curved surface of the white dwarf, the illumination is decreasing, with slightly more than the square of the distance from the axis of the post-shock region. Further, albedo varies as a function of temperature. Although the effects of irradiating a white dwarf atmosphere have been explored to some extent (Williams et al 1987, Heise 1995), this is an area which needs further work to determine how the temperature of the reprocessed spectrum is effected by parameters such as the accretion rate and magnetic field.

We note, however, that higher specific accretion rates result in lower shock heights, and higher magnetic fields also reduce the height of the post-shock region (see for example Cropper et al 1999), so the solid angle of emission from the post-shock flow intercepted by the white dwarf photosphere is increased. In these high-state data of CE Gru, we have no reason to expect anomalously low specific accretion rates, and CE Gru has a magnetic field strength typical of polars. Therefore there is no obvious reason for the reprocessed component to have moved into the EUV if it is normally in the soft X-ray band in polars. This gives support to the Heise & Verbunt (1988) suggestion that the soft X-ray component is indeed caused by blobby accretion.

Some factor(s) must determine the number, length and density of blobs. Obvious parameters include the magnetic field strength and orientation of the white dwarf, the orbital period and the mass transfer rate. Ramsay et al (1994) identified the magnetic field strength as one important parameter. Further progress in this regard awaits a systematic analysis of the strength of the soft X-ray component as a function of these parameters in a sufficiently large sample of polars.

REFERENCES

Aizu, K., 1973, prog Thei Phys, 49, 1184

Cropper, M., Bailey, J. A., Wickramasinghe, D. T., Ferrario, L., 1990, MNRAS, 244, P34

Cropper, M., Wu, K., Ramsay, G., Kocabiyik, A., 1999, MNRAS, 306, 684

Cropper, M., Wu, K., Ramsay, G., 2000, New Astronomy Reviews, 44, 57

den Herder, J. W., et al, 2001, A&A, 365, L7

Frank, J., King, A. R., Lasota, J. -P., 1988, A&A, 193, 113

Gänsicke, B., Beuermann, K., & D. de Martino, 1995, A&A, 303, 127

Hawkins, M. R. S., 1981, Nature, 293, 116

Hawkins, M. R. S., 1983, Nature, 301, 688

Heise, J., Verbunt, F., 1988, A&A, 189, 112

Heise, J., 1995, In Cape Workshop on Magnetic cataclysmic variables, ASP Conf Ser, 85, Ed. D. A. H. Buckley & B. Warner, 162

Ishida, M., Matsuzaki, K., Fujimoto, R., Mukai, K., Osborne, J. P., 1997, MNRAS, 287, 651

King, A. R., Lasota, J. P., 1979, MNRAS, 188, 653

Kuijpers, J., Pringle, J. E., 1982, A&A, 114, L4

Lamb, D. Q., Masters, A. R., 1979, ApJ, 234, 117

Mason, K. O., et al 2001, A&A, 365, L36

Nauenberg, M., 1972, ApJ, 175, 417

Osborne, J., 1988, Societa Astronomica Italiana, Memorie, vol. 59, no. 1-2, 117

Ramsay, G., Mason, K. O., Cropper, M., Watson, M. G., Clayton, K. L., 1994, MNRAS, 270, 692

Ramsay, G., 2000, MNRAS, 314, 403

Ramsay, G., Cropper, M., Cordova, F., Mason, K., Much, R., Pandel, D., Shirey, R., 2001, MNRAS, 326, L27

Ramsay, G., Cropper, M., 2002, submitted, MNRAS

Strüder, L., et al, 2001, 365, L18

Tuohy, I. R., Ferrario, L., Wickramasinghe, D. T., Hawkins, M. R. S., 1988, ApJ, 328, L59

Turner, M., et al 2001, A&A, 365, L27

Verbunt, F., Bunk, W. H., Ritter, H., Pfeffermann, E., 1997, A&A, 327, 602

Watson, M. G., King, A. R., Jones, M. H., Motch, C., 1989, 237, 299

Wickramasinghe, D., Ferrario, L., Cropper, M., Bailey, J., 1991, MNRAS, 251, 137

Williams, G., King, A. R., Brooker, J. R. E., 1987, MNRAS, 226, 725